9-1-1990

Experimental performance of a binary phase-only optical correlator using visual and infrared imagery

Samuel Peter Kozaitis

Sandra L. Halby

Wesley E. Foor

PROCEEDINGS OF SPIE

SPIEDigitalLibrary.org/conference-proceedings-of-spie

Experimental performance of a binary phase-only optical correlator using visual and infrared imagery

Samuel Peter Kozaitis
Sandra L. Halby
Wesley E. Foor

SPIE.

Experimental performance of a binary phase-only optical correlator using visual and infrared imagery

S.P. Kozaitis

Florida Institute of Technology, Department of Electrical and Computer Engineering
150 W. University Blvd., Melbourne, FL 32901-6988

S. Halby and W. Foor

Rome Air Development Center, Photonics Laboratory
Griffiss AFB, NY 13441

ABSTRACT

Experimental results of an optical binary phase-only correlator using both visual and IR imagery are presented. The inputs to the correlator originate from actual aerial imagery containing aircraft and a variety of distortions. Filters used as a database for the system are derived from models of aircraft. Digital image processing techniques are used on images before being input into the optical correlator to enhance the performance of the system. Both noise removing and segmentation techniques are investigated. Input images to the correlator are displayed on a 128x128 magneto-optic spatial light modulator (SLM). Experimental results are presented which show that the system performs well with images which are easily segmented from the background.

1. INTRODUCTION

Autocorrelation experiments have shown that a binary phase-only filter (BPOF) in an optical correlator performs better than a matched filter [1]. Furthermore, it has been shown that an optical correlator using a BPOF produces a narrow and sharp correlation peak, and that experimental results generally agree with computer simulations.

This paper presents experimental results of a BPOF optical correlator using infrared (IR) and visual imagery. Images used in the correlator originate from high-resolution aerial photographs of airfields. They contain a variety of aircraft and distortions, including scan lines, noise, and clutter. Portions of these photographs are displayed on a 128x128 pixel magnetooptic spatial light modulator (SLM) as inputs to the optical correlator. Filters which act as a database for the system were derived from models of aircraft generated in the laboratory. The results of these experiments help evaluate binary phase-only filtering for pattern recognition using real-world imagery.

Digital image processing techniques are used to convert the aerial imagery to binary form for display on an SLM. Several algorithms are examined for noise reduction and segmentation. The image processing techniques are not intended to be exhaustive. Relatively simple preprocessing algorithms are being examined to identify methods useful for a BPOF optical correlator.

An optical correlator is used here which employs a filter SLM with a reduced spatial resolution when compared to the input SLM. This configuration can significantly decrease the cost of the system and potentially increase the speed. Optical correlation is described in the next section followed by a description of the image processing techniques used, the optical system and

experimental results.

2. OPTICAL CORRELATION

A BPOF is used here because it results in a higher and narrower correlation peak and improved discrimination in comparison to the matched filter; however, the BPOF is relatively sensitive to distortion including scale and rotation changes. In addition, a BPOF can be implemented with a magnetooptic SLM relatively easily.

Since the SLMs used here were limited to binary operation, both the input images and filters needed to be converted to a binary form. The conversion technique for input images is described in the next section. Filters for the correlator were generated as follows. The Fourier transform of a desired image was computed and its phase was set to either 0 or π at each pixel. If the calculated phase angle was between 0 and π, then the phase at that pixel was set to 0. If the calculated phase angle was between π and 2π, then the phase at that pixel was set to π. Other methods have been employed to create a BPOF where the threshold phase angle may lie at different axes [2,3].

Computer simulation of correlation experiments were performed using a 128x128 point FFT algorithm. Our experiments used a correlator with a 48x48 SLM in the filter plane which is discussed in section five. The 128x128 filters were created then averaged to obtain a 48x48 filter.

Database images used in the correlator were taken from models of aircraft. A typical database image is shown in Fig. 1 which is the outline of an aircraft. A computer simulation of the autocorrelation of the image in Fig. 1 using a 128x128 input and a 48x48 filter is shown in Fig. 2. The sharp correlation peak associated with BPOFs is easily identified. When the image in Fig.1 is filled in such that a silhouette of an aircraft exists, its autocorrelation result is almost identical to that of Fig. 2. The only difference is that the base of the correlation peak is slightly wider.

There is more than one definition of signal-to-noise ratio (SNR). We will use the following definition as the SNR [4]

$$SNR = I_{max}\left(\sum_{n=1}^{N}\frac{I^2_{<0.5Imax}}{N}\right)^{-1/2} = \frac{I_{max}}{rms(I_{<0.5Imax})} \qquad (1)$$

where N is the number of noise pixels and (rms) is the root mean square. The SNR is the ratio of the maximum intensity of the correlation peak divided by the rms value of all pixels below half the height of the correlation peak. The values of pixels used in the denominator of Eq. 1 are referred to as noise in the correlation plane.

The SNR as defined by Kallman [5] is also useful and will be used here and referred to as the signal-to-clutter ratio (S/C). The S/C can be thought of as the ratio of the lowest peak of an in-class object to the largest peak of an out-of-class object.

3 IMAGE PROCESSING

Digital image processing techniques were used to convert high-resolution visual and IR aerial photographs to binary form for display on a SLM as an input to the optical correlator. The images consisted primarily of an airfield with a variety objects, distortions, and clutter. They were digitized with 8 bits/pixel and stored on a computer for further processing. The digitized images were examined in 128x128 sections for implementation on the SLM and processed with algorithms primarily used for noise removal and segmentation.

Noise removing algorithms are often based on averaging. A problem with averaging filters is that they smear edges. Therefore, nonlinear filters have been developed to filter noise, but at the same time preserve both lines and edges in an image. Either linear or nonlinear filters may work best for a particular type of noise. Therefore, nonlinear filters have been developed which have characteristics of both linear and nonlinear filters [6].

Noise removing filters used for preprocessing images for a binary phase-only optical correlator have been shown to often give a small but noticeable improvement [7]. In our experiments we used an adaptive mean filter for noise filtering [6]. It can be described as

$$Y=\frac{\sum_{i=1}^{N} a(i)X(i)}{\sum_{i=1}^{N} a(i)} \qquad (2)$$

where a(i) is a weight function described by

$$a(i)= \begin{cases} 1, & \text{if } |X(i)-X(A)| < q \\ 0, & \text{otherwise} \end{cases} \qquad (3)$$

A 3x3 window is considered here; however, the filter applies to all size windows. The nine pixels within the window can be represented by X(i) where i varies from 1 to 9, and X(A) is the average of the pixel values in the window. The number of pixel values used in averaging is not constant. The size and shape of the window adjusts automatically depending on the signal. A pixel value is included in the averaging if the difference between itself and the mean value of the window is less than a threshold q.

The filter works best when the standard deviation of the noise in an image is known. The value q can be chosen according to some optimization criterion that equals 3σ, where σ is the standard deviation of the noise [6]. The noise statistics of an image may be estimated from taking two images of the same scene [8]. In our experiments we had to estimate the standard deviation of the noise because our images originally came from photographs.

Since gray-level images were used, a threshold value ultimately had to be chosen to obtain a binary image. Often a thresholding operation is used to segment an image. Segmentation is the process of separating objects of interest from a background. When it is obvious what the object and background are such as in Fig. 4c, then a threshold value may be easily chosen. A threshold value for an image can be automatically chosen based on the noise statistics of an image, by an isodata technique which is based on the analysis of a histogram, or by simply choosing a fixed value near the middle of the available pixel values [8]. The resulting image often results in an image which is similar to the silhouette of the object if the threshold value was chosen properly. When the segmentation is not as simple as in Fig. 4c, edge-based segmentation is often used.

There are several types of edge detection algorithms. A popular algorithm is the Sobel edge detector. It is used in our experiments to segment an object from a background because of its good performance. The resulting image usually resembles the outline of the object. Although the silhouette of an object and its outline look different they have a similar frequency content.

4. OPTICAL SYSTEM

The experimental set up consisted of an optical correlator with two Semetex magnetooptic SLMs in both the input and Fourier planes. A computer was used to obtain digitized images from aerial photographs and process the images as described in the previous section. A computer also drove both filter and input SLMs. A camera was placed in the correlation plane to examine the output of the system.

The SLM in the input plane was a 128x128 pixel device, and the SLM in the filter plane was a 48x48 device. In computer simulations, the correlator with a 48x48 filter performed almost exactly the same as the 128x128 device. The system is aligned using the same procedure as if the SLMs had the same resolution. The highest spatial frequency of the input SLM is aligned with the edge of the filter SLM.

The use of a filter SLM with lower spatial resolution than the input SLM can have several advantages. An important practical consideration is that the cost of the filter SLM is about one-third the price of the input SLM for our magnetooptic devices. This fact can significantly reduce the cost of a system when compared to two 128x128 magnetooptic SLMs.

Another advantage is that the length of the system may often be made shorter, the amount depending on the specific SLMs being used. The focal length of the correlator is given as [9]

$$f = \frac{N_2 d_1 d_2}{\lambda}, \qquad (4)$$

where N_2 is the number of pixels along a side of the filter SLM, d_1 and d_2 are the pixel sizes of the input and filter plane SLMs respectively, and λ is the wavelength of the light being used. The focal length of the system if proportional to the resolution of the filter SLM if other factors remain constant.

In our correlator, the length savings was not as dramatic as could be, because the pixel size

of the filter SLM was larger than that of the input SLM. Furthermore, we used a configuration similar to that of a 2f correlator [10]. The length of the system measured from the input SLM to the correlation plane was 1.6m. Had two 128x128 SLMs been used in a 2f configuration, the system would be 2.2m long.

Another advantage of a reduced-resolution SLM in the filter plane is the potential for faster operation. Because less data would be transferred for an electrically addressed device, the possibility for more frames to be transferred given a constant data rate exists. The frame rate of an SLM may rely on a number of factors depending on the specific SLM. The faster frame rate did not apply to our device because its speed is not limited by the data rate of the computer.

5 EXPERIMENTAL RESULTS

A variety of visual and IR images containing different aircraft were used as inputs to the optical correlator. These images were correlated against a database of several different aircraft. The filters for the database were generated by digitizing images of models of several aircraft. Images were generated which contained both the silhouette and edge enhanced versions of the models. In addition, images containing edges of different widths were generated. Filters were then made from these images using the technique described in section two.

Autocorrelations of images used in the database produced sharp correlation peaks which agreed well with computer simulations. An example of the experimental autocorrelation of the image in Fig.1 is shown in Fig. 3. The SNR as defined earlier is 69.6 or 18.4db, and the S/C=10.9 db. As can be seen by comparing the autocorrelation result with Fig. 2, the correlator produces results which agree with simulation. The result shown in Fig. 3 is used as a reference for other correlation results using the filter derived from Fig.1.

Many different input scenes were used as inputs to the correlator. Several examples are shown in Fig 4a-f. There are distortions in all the images in Fig. 4. Some are not as apparent as others due to the printing used here. For example, scan lines are visible in some of the images. The nose of the aircraft in Fig. 4a tends to fade into the background, and the fuselage is fuzzy. These factors make it difficult to define exactly where an edge should be. Additional difficulties arise in Fig. 4f, for example, the leading edge of the wing is barely visible. In Fig. 4c, each wing appears to make a different angle with the fuselage. The result of these distortions is that the input scene to the correlator will rarely be the same as an image in the database.

Correlation results using edge-enhanced inputs using the Sobel operator, were compared in terms of the thickness of the edges used. Inputs with edges varying from 1 to 5 pixels were used with corresponding filters. Sharp correlation peaks for single-pixel edges were obtained, but the results were noisy. The best results were obtained with edge-detected images using edges of three pixels in width. The correlation peaks were a little broader but easier to obtain than with single-pixel edges. Images with thicker than three-pixel edges showed a degradation of results. Silhouetted imagery showed very similar results to that of the best edge-detected imagery.

Experimental results of correlations of input scenes from Fig. 4 with a filter of Fig. 1 are described below. The filter is the same type of aircraft as in both Figs. 4a and 4b. The inputs were preprocessed with an adaptive mean filter, followed by a Sobel edge detection and, finally with a thresholding operation. The thresholding was performed by an isodata method. In this method, the histogram of the edge-enhanced image is examined. A threshold value is chosen to lie between peaks in the histogram. This method works best when there are both strong and weak

edges in the image. The strong edges are usually retained while the weak edges are eliminated. The experimental result of the correlation of the image in Fig. 4a and the filter in Fig. 1 is shown in Fig 5. Here a correlation peak is observed which is slightly broader than the autocorrelation result in Fig. 2. The height of the peak is about 30% the height of the experimental autocorrelation of Fig. 3. The SNR is 25.8 or 14.1db, and the S/C is 2.6db. This result was typical for images where an aircraft is relatively easily separated from the background.

The result using the input image in Fig. 4b and the filter in Fig.1 is shown in Fig. 6, The result shows that the SNR is 20.2 or 13.1db, and the S/C is 2.4 db. Figure 7 shows the experimental results using Fig. 4c as an input and the same filter. Here the input and filter are of different types of aircraft. The noise peaks are the same height as the correlation peak and the S/C is near 0. The results in Figs. 5-7 are on the same scale and are not normalized.

An additional consideration in our system was the light throughput. The SLMs were highly attenuating so only a small fraction of the incident light reached the correlation plane. The attenuation of the SLMs was constant, so the amount of light arriving at the correlation plane is proportional to the number of "on" pixels in the input SLM. As images with thicker edges were used, more light was available in the correlation plane.

6 CONCLUSION

Digital image processing techniques are useful for converting distorted gray-level aerial imagery to binary images for use in an optical correlator. Models of aircraft used to generate filters give satisfactory results. Both edge detection and silhouetting operations for segmenting an object from a scene also produce good results. Thin edges tend to produce noisy results, and thick edges produce broad correlation peaks, with edges of three pixels giving the best result. SNRs of over 20db were common, which correspond to S/C ratios in the vicinity of 3db. The resulting correlation peaks were about 30% the height of the autocorrelation peak of the database image. The results presented here show that a BPOF optical correlator using digital image preprocessing techniques is useful for ground exploitation.

7 ACKNOWLEDGEMENT

This work was performed in the Photonics Laboratory of the Rome Air Development Center at Griffiss AFB, NY.

8 REFERENCES

[1] M.A. Flavin, and J.L. Horner, "Correlation experiments with a binary phase-only filter implemented on a quartz substrate," Opt. Eng. 28, 470 (1989)

[2] D.M. Cottrell, R.A. Lilley, J.A. Davis, and T. Day, "Optical correlator performance of binary phase-only filters using Fourier and Hartley transforms," Appl. Opt. 26, 3755 (1987)

[3] M.W. Farn, and J.W. Goodman, "Optimal binary phase-only matched filters," Appl. Opt. 27, 4431 (1988)

[4] M.A. Flavin, and J.L. Horner, "Amplitude encoded phase-only filters," Appl. Opt. 28, 1692 (1989)

[5] R.R. Kallman, "Optimal low noise phase-only and binary phase-only correltion detectors for correlation filters," Appl. Opt. 25 4216 (1986)

[6] Y-S. Fong, C.A. Pomalaza-Raez, and X-H. Wang, "Comparison study of nonlinear filters in image processing applications," Opt. Eng. 28, 749 (1989)

[7] S.P. Kozaitis, and A. Roeksabutr, "Image preprocessing for phase-only filtering," SPIE 1151, 154 (1989)

[8] J.F. Haddon, "Generalised threshold selection for edge detection," Pattern Recognition 21, 195 (1988)

[9] J.A. Davis, W.A. Waring, G.W. Bach, R.A. Lilley, and D.M. Cottrell, "Compact optical correlator design," Appl. Opt. 28, 10 (1989)

[10] J.L. Horner, and C.K. Makekau, "Two-focal length optical correlator," Appl. Opt. 28, 5199 (1989)

Fig.1 Sample of image in database

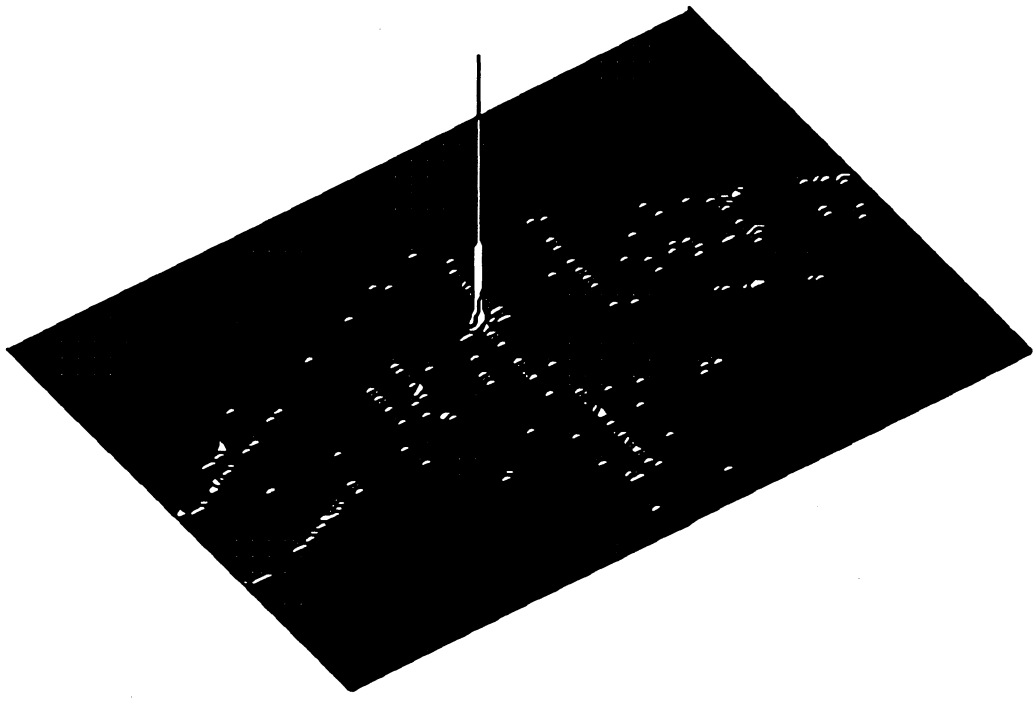

Fig.2 computer simulation of autocorrelation of Fig.1 using a 128x128 input image and a 48x48 filter

Fig. 3 Experimental result of autocorrelation of Fig. 1.

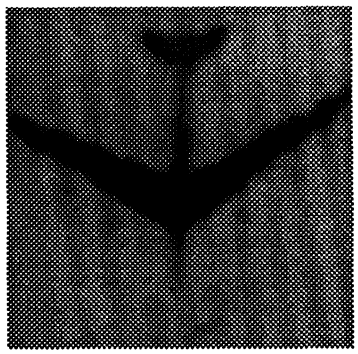

a

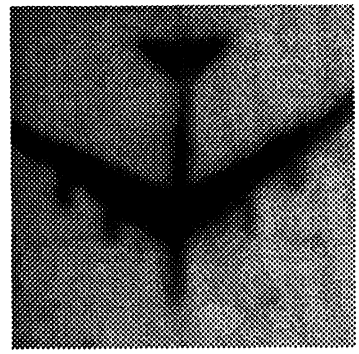

b

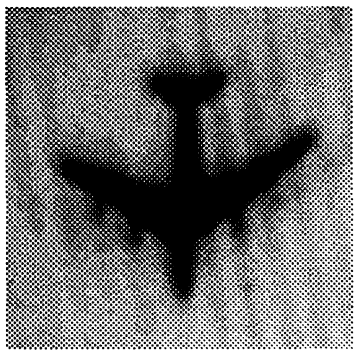

c

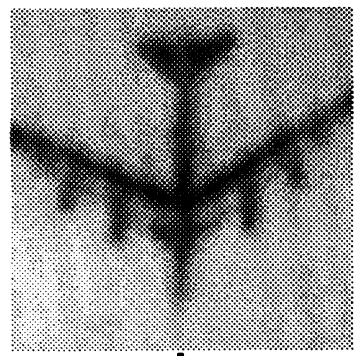

d

e

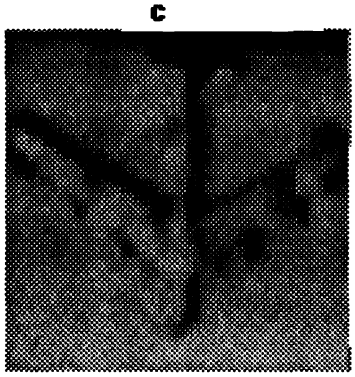

Fig 4

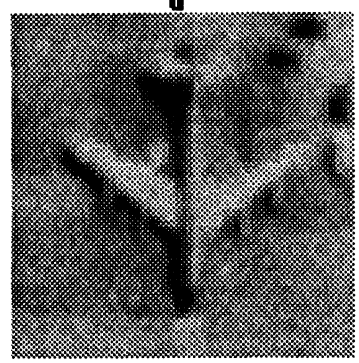

f

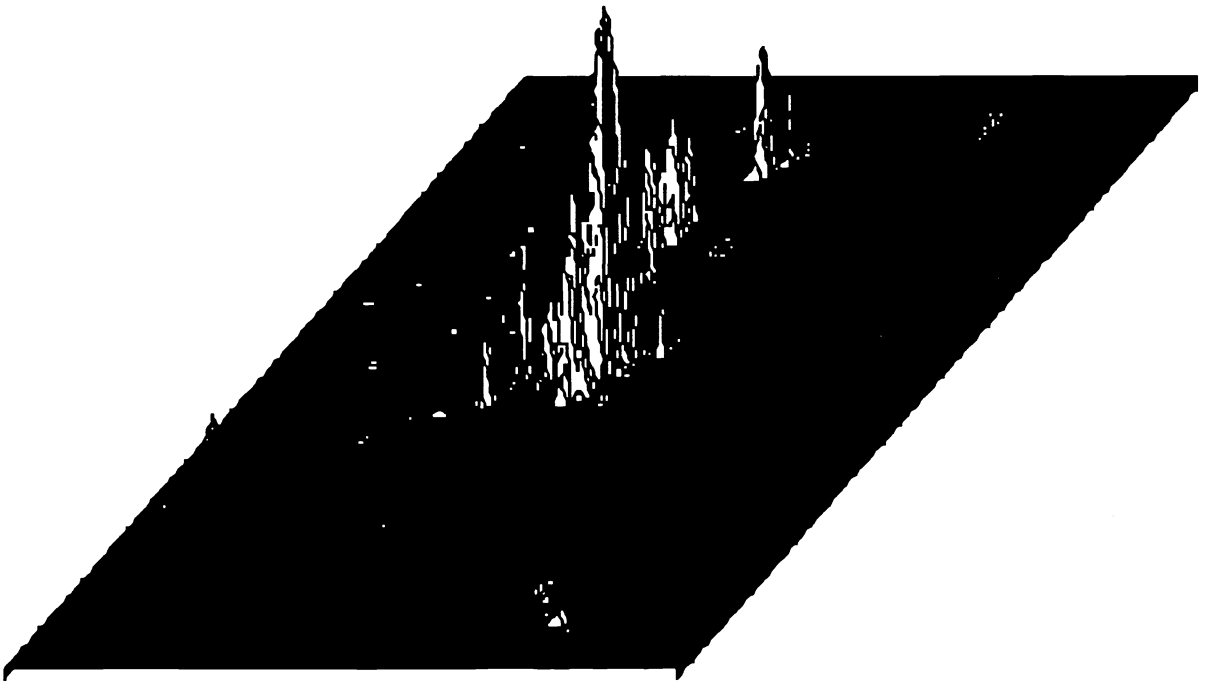

Fig. 5 Experimental correlation results of image in Fig. 4a and filter of Fig. 1

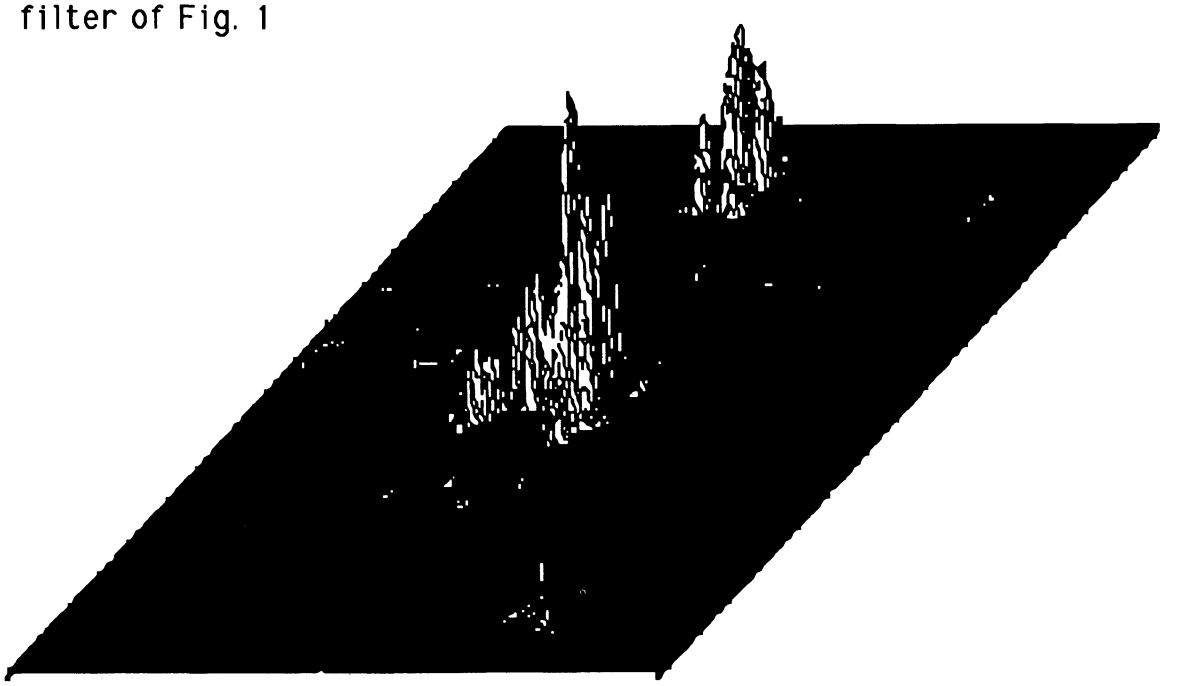

Fig. 6 Experimental correlation results of image in Fig. 4b and filter of Fig. 1

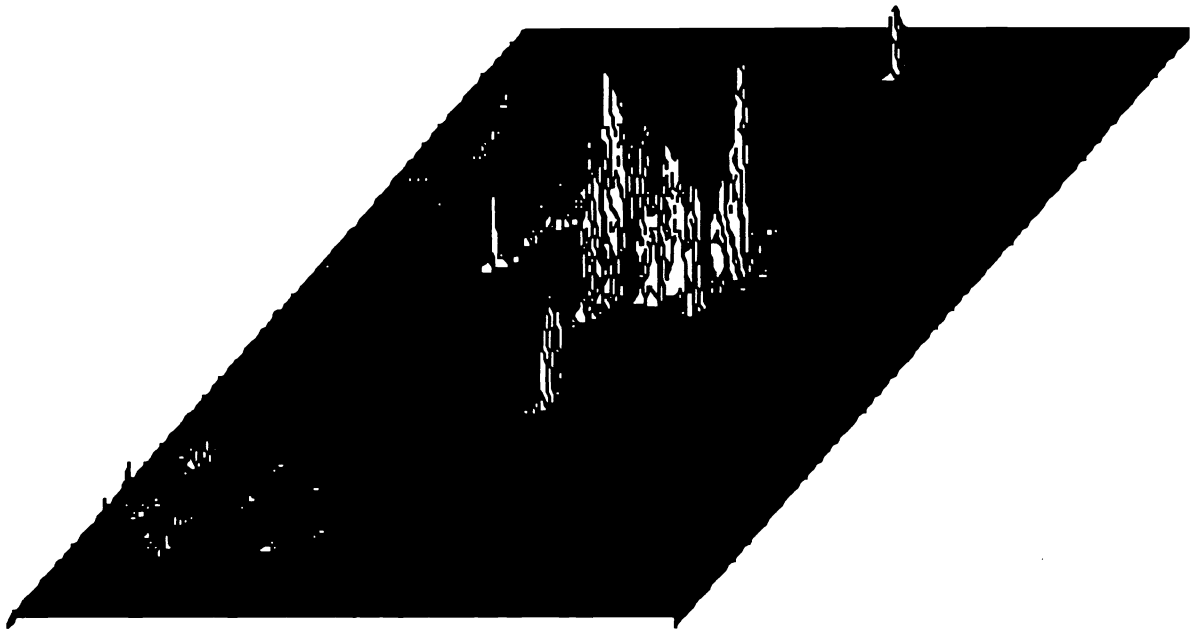

Fig. 7 Experimental correlation results of image in Fig. 4c and filter of Fig. 1